(article starts on next page)

Research Paper

Speciation of Zn in WtE fly ash residues after wet treatment

Karin Karlfeldt Fedje [a,b] , Ivana Staničić [c] , Charlotte Nilsson [d] , Fanny Bergman [e,f] ,
Haakon M. Rui [g] , Inge Johansson [g] , Simone Sala [h] , Jenny Rissler [e,f,*]

[a] Department of Architecture and Civil Engineering, Chalmers University of Technology, SE-412 96 Gothenburg, Sweden
[b] Recycling and Waste Management, Renova AB, Box 156, SE-401 22 Gothenburg, Sweden
[c] Department of Space, Earth and Environment, Chalmers University of Technology, Chalmersplatsen 4, Gothenburg SE-41296, Sweden
[d] Fortum Waste Solutions AB, SE-69285 Kumla, Sweden
[e] Ergonomics and Aerosol Technology, Lund University, SE-22100 Lund, Sweden
[f] NanoLund, Lund University, SE-22100 Lund Sweden
[g] NOAH AS, 3081 Holmestrand, Norway
[h] RISE Research Institutes of Sweden, SE-22370 Lund, Sweden

1. Introduction

Municipal solid waste (MSW) volumes continue to increase. At a global scale, MSW is estimated to equal 3.8 billion tons annually by 2050 (United Nations Environment and Association, 2024). Non-recyclable MSW is commonly processed in waste-to-energy (WtE) facilities, allowing for recovery of energy while reducing waste volumes. WtE generates fly ash (FA) enriched in metals and inorganic compounds (Quina et al., 2018). Due to the presence of potentially toxic species, FA is typically considered hazardous waste and is disposed of in specialised landfills at high cost. However, the metal-enriched FA can be seen as a metal resource. One option for recovering metals is acid-leaching, where soluble species are separated into a liquid phase for further processing. Recovery processes for metals, mainly Zn, have been developed using this approach (Karlfeldt Fedje and Andersson, 2020; Rasmussen, 2015; Schlumberger et al., 2007). Another approach for utilising the ash is to reduce metal leachability through stabilisation at a slightly alkaline pH, since several metal ions have their mobility minimum at pH values of approximately 9–11, see e.g. (de Repentigny et al., 2018). Fly ashes with added lime are typically more suitable for this treatment, whereas ashes without lime addition are more suitable for acid-leaching.

While stabilised ash could potentially be used for construction purposes (Ferreira et al., 2003; Liang et al., 2023), the ash residue after acid-leaching is landfilled if not further treated. However, for both ash residues, avoiding unintentional metal leaching is essential. Leachability depends on the chemical form of the element. The current understanding of how acid-leaching and stabilisation affect chemical contents and forms, as well as the particle surfaces in FA, is limited, which may restrict its secondary use. One reason for the limited understanding is the lack of analytical methods for determining the chemical form of low-

concentrated (<1 wt%) elements. While conventional techniques, such as X-ray powder diffraction (XRD), provide speciation of the main crystalline species, they are rarely sensitive enough for characterising low-concentration elements and do not allow speciation of amorphous constituents. One technique with high potential to determine the chemical form of low-concentrated elements in the complex ash matrix is X-ray Absorption Near Edge Structure (XANES) spectroscopy, see e.g. (De Matteis et al., 2024; Rissler et al., 2024, 2020; Scholz et al., 2024; Struis et al., 2004).

XANES provides detailed information on the oxidation state and local electronic environment of a specific target atom by analysing the spectral fine structure near the absorption edge of the target atom, without the disturbance of other elements that are not chemically bound to the target atom. XANES is a powerful tool for probing the chemical composition, changes in bonding and coordination, and structural variations of low-concentration elements in complex materials, even within heterogeneous and amorphous samples. Typical XANES detection limits range from a few ppm to just below percent levels, depending on factors such as target element, sample matrix, photon flux, beamline configuration (including detector), and data acquisition time. Due to the complexity of modelling XANES spectra, interpretation and identification of chemical forms requires comparison with appropriate reference materials. Furthermore, the more complex the speciation of the target element is, the more uncertain the interpretation of the spectra will be. While XANES is a bulk technique, X-ray photoelectron spectroscopy (XPS) is a surface-sensitive technique that provides both elemental and chemical state information of the outer surface, typically the outmost atomic layers, of solid samples. A key advantage of this method is its low detection limit, which reaches the parts per thousand range. Several authors have employed XPS to investigate the chemical speciation of

metals such as Cu, Pb, and Zn in fly and bottom ashes. For example, XPS has been used to monitor the chemical speciation of metals in FA (Chuai et al., 2022; Wu et al., 2023), and to reveal interactions between bed materials and metals such as Cu, Pb, and Zn in bottom ash (Staničić et al., 2022) – highlighting also XPS as a valuable tool for investigating the complex chemistry of ashes. An advantage of using XANES and XPS is that both are non-destructive methods.

This paper aims to investigate how acid-leached and gypsum-stabilised FA residues from WtE facilities differ from each other and the corresponding untreated ashes in terms of Zn chemical form and leaching. This study provides a comprehensive view of Zn speciation, offering a deeper understanding of Zn distribution at particle surfaces and bulk FA, as well as how different treatment methods influence this distribution. Knowledge about Zn speciation and distribution in wet-treated WtE FA residues is very limited. Through this work, a better understanding of Zn behaviour in ash is reached, and it contributes to facilitating increased circularity through improved Zn recovery or the safe secondary use of treated FA.

2. Materials and methods

Within this study, both untreated and treated FA samples were investigated. Untreated samples (GB2, GB4, and GB5) were collected as electrostatic filter ash from three full-scale grate-fired WtE boilers in Sweden and Denmark. All three facilities treat between 400 000 and 600 000 tons of waste annually, and have been previously described in (Rissler et al., 2024). Ash samples GB2 and GB5 were collected directly from the hoppers, while GB4 was collected from the ash silo. Additionally, an air pollution control (APC) ash sample with the addition of slaked lime (Ca(OH)$_2$) was collected from the same plant as sample GB2 and is herein referred to as GB2APC. GB2APC was collected manually from the top of the bulk transport as it arrived at the treatment plant; the rest of the material was discharged into a silo. All samples were collected as several subsamples, which were then mixed into a single sample of at least 500 g for each facility. The ashes were collected under stable and normal incineration conditions to ensure they accurately represent the standard conditions. Thereafter, the samples were packed in airtight containers until further treatment. The chemical composition of the original ash samples (previously reported in Rissler et al., 2024) is given in the Supplementary Materials, Table S1.

The procedures for obtaining the treated ash samples are described in subsection 2.1, followed by the analytical methods applied in this study in subsections 2.2–2.5.

2.1. Ash treatment methods

The FA samples were subjected to wet treatment, i.e., stabilisation at alkaline pH or leaching at acidic pH, as schematically represented in Fig. 1. Stabilisation via gypsum formation was applied to GB2APC, as this ash had added lime, which is advantageous for stabilisation. The resulting residue is referred to as GB2APCg. This sample originates from the full-scale stabilisation process at the Langøya site (Rui et al., 2021). Acid-leaching was used for GB2, GB4, and GB5, as these samples had no lime addition. The acid-leaching was carried out in one cycle for GB5 and three cycles for GB2 and GB4. The resulting residues are referred to as GB2a, GB4a, and GB5a, respectively. All treated ash samples were dried and stored in air-tight containers until further analysis.

The one-cycle method is a lab-scale version of the full-scale process used in the plant where GB5 was collected (Renova AB, 2023), while the three-cycle method is at laboratory scale, with potential for further development to full-scale. Ash GB5 has been thoroughly studied previously in terms of Zn leaching and recovery, with a conclusion that approximately 70 % of the Zn can be leached from the ash (Karlfeldt Fedje and Andersson, 2020). The total amount analyses, as shown in Table S1, and earlier research on GB2, GB4, and GB5 (Rissler et al., 2024) indicate that Zn is bound in more stable compounds, such as
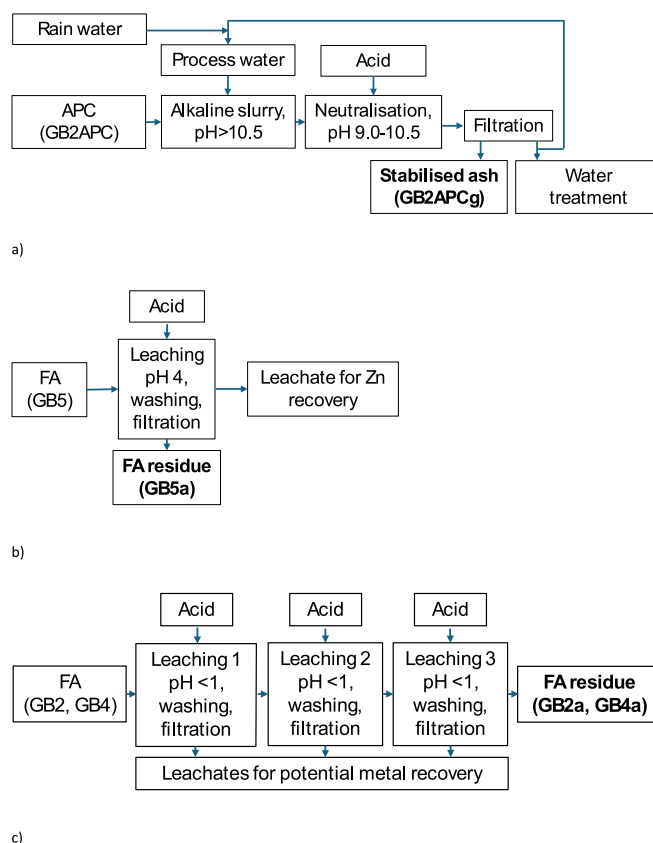

Fig. 1. Schematic representation of the three ash treatment methods used: a) stabilisation, original ash GB2APC and residue GB2APCg; b) acid-leaching, one cycle, original ash GB5 and residue GB5a; c) acid-leaching, three cycles, original samples GB2 and GB4 and residues GB2a and GB4a. Acid: H$_2$SO$_4$ (a) and HCl (b and c), Process water: re-circulated water from the neutralisation process, Alkaline slurry: Mixture of ash and process/rain water to start the neutralisation process, Neutralisation: Addition of waste acid to the alkaline slurry to reach pH for minimising metal mobilisation, Filtration: Dewatering of the ash residues. The collected liquids are sent to further water treatment (a) or for metal recovery (b and c). Washing: Ash samples GB2, GB4, and GB5 are washed with deionised water before filtration. Leaching: HCl leaching in one (b) or three (c) steps at pH 4 or < 1, respectively.

silicates and Fe/Al oxides, in GB2 and GB4 compared to GB5. Thus, a more rigorous acid-leaching may be necessary to achieve similar or higher Zn mobility than from GB5. GB2 and GB4 are similar but generated from WtE plants in Sweden and Denmark, respectively, with variations in, e.g. waste composition that might influence the Zn speciation.

2.1.1. Stabilisation

Sample GB2APC was mixed with recirculated process water and stored rainwater to make an alkaline ash slurry, as shown in Fig. 1a. This slurry was then used to increase the pH of spent sulfuric acid (H$_2$SO$_4$, approximately 25 wt%) originating from titanium dioxide (TiO$_2$) manufacturing. The reaction was stepwise, with a total residence time of ca 90 min. The process was controlled to maintain pH levels between 9.0 and 10.5, aiming to achieve the lowest mobility for targeted hazardous elements, such as Cd, Cu, Pb, and Zn. The process generated a gypsum matrix from the reaction of Ca from the ash with sulphate from the sulfuric acid. The gypsum matrix was dewatered in a filter press, and the separated water was recirculated as process water to generate the ash slurry.

2.1.2. Acid-leaching

2.1.2.1. One cycle. The treated ash sample GB5a was prepared in a laboratory-scale experiment, starting from 10 g of untreated FA (GB5) and following a procedure comparable to that used in the full-scale plant. Details about the process in the pilot tests and the full-scale plant can be found in (Renova, 2023; Karlfeldt Fedje and Andersson, 2020). For the laboratory experiment, acid (mainly HCl, pH 0 i.e. 1 M, Supplementary Materials, Table S2) was collected from the wet flue gas cleaning treatment in the full-scale WtE plant from which GB5 ash originated and used to leach the FA with a liquid-to-solid ratio of about 3.5 at pH 4 for approximately 10 min, as demonstrated in Fig. 1b. The ash residue was separated from the liquid via filtration, washed (18.2 MΩ deionised water) and dewatered, while the ash leachate was pH adjusted to around 10 to precipitate the Zn product. The resulting water was treated in the ordinary wastewater treatment system.

2.1.2.2. Three cycles. Samples of approximately 200 g of ash GB2 and GB4 were treated according to the process outlined in Fig. 1c. Briefly, the samples were extracted in three consecutive cycles of acid-leaching (30 min, 5.5 % HCl, pH < 1 for each cycle) followed by rinsing with 18.2 MΩ deionised water. Following each step, the solid phase was separated from the liquid by high-pressure (800 kPa) filtration before transfer to the next step.

2.2. Sequential extraction

The potential mobility of Zn in untreated and treated ash samples was assessed by a sequential extraction procedure developed by (Tessier et al., 1979) and further modified by (Karlsson et al., 1988). All samples were extracted in five consecutive steps using increasingly aggressive extractants. The targeted fractions and extractants used for each step were: 1) Loosely bound species, extracted with de-ionized water (18.2 MΩ); 2) Exchangeable species, extracted using 1 M NH_4OAc, pH 7; 3) Carbonates and easily soluble hydroxides, extracted with 1 M NH_4OAc, adjusted to pH 5 using acetic acid; 4) Reducible fraction (oxides), extracted with 0.04 M NH_3OHCl in 25 % acetic acid, and 5) Oxidizable fraction, extracted using H_2O_2 and HNO_3. In the text, these steps are referred to as MQ, Ac7, Ac5, Red and Ox, respectively. The residue remaining after the last step is referred to as Res. The reducible and oxidizable fractions were extracted at elevated temperatures (96 °C and 85 °C, respectively), while fractions 1–3 were extracted at room temperature (20 °C). Following each sequence step, the solids were separated from the liquid by centrifugation (4000 RPM, 10 min) before being transferred to the next step. All extractions were performed using a liquid-to-solid ratio of 20, and the initial ash weight was 0.5 g per sample, representing 100 % dry substance. Sample dilution and preparation of all solutions were done using deionized water (18.2 MΩ) and analytical-grade chemicals.

2.3. XANES

XANES analysis was performed at the Balder beamline at the 3 GeV ring (operated at ~400 mA) of MAX IV Laboratory (Klementiev et al., 2016; Robert et al., 2023). The XANES scanning was performed around the Zn K–edge at 9659 eV, focusing on Zn speciation. To obtain samples compatible with XANES, each sample was mixed with boron nitride (BN) and pressed into tablets (Rissler et al., 2020). For each tablet, a sample of ~100 mg ash was used. For the fresh ash, the samples were not ground or pressed into tablets, as we have observed that the preparation method affects Zn speciation (Rissler et al., 2024). A beam size of H 100 × V 100 μm^2 was used, and sequential scans were performed by moving the beam in steps of 200 μm over the sample to minimise the effects of beam damage. The energy was set by the monochromator (cryogenically cooled Si(111) crystals) and calibrated by assigning the first peak of the

first derivative for the K–edge of a Zn metal foil to 9659 eV. The spectra were collected primarily in transmission mode. For the lowest-concentration samples (typically when Zn < 0.5 wt%, but sample-dependent), the fluorescence mode with a passivated implanted planar silicon (PIPS) detector was used to enhance sensitivity. Data processing and normalisation were completed using Athena software (Ravel and Newville, 2005), enabling the linear combination fitting (LCF) of the spectra from a large set of references. The implementation of LCF is described in (Rissler et al., 2020). In this study, except for GB2APC, the same untreated ashes were used as in the previously published study, and thus the results from the LCF of GB2, GB4 and GB5 are identical to the results found in Table 3 in (Rissler et al., 2024): they are included here for comparison purposes.

In this study, the same set of references as presented in the study by (Rissler et al., 2024) was used: $KZnCl_3$, K_2ZnCl_4, $CaZnCl_4$, $ZnCl_2$, $Zn_5(OH)_8Cl_2·H_2O$, $ZnBr_2$, ZnO, $Zn(OH)_2$, Zn_2O, ZnOOH, $Zn_3(PO_4)_2 · 4 H_2O$, $ZnNO_3 · 6 H_2O$, $Zn_5(CO_3)_2(OH)_6$, $ZnCO_3$, $ZnSO_4·H_2O$, ZnS, $Zn_4Si_2O_7(OH)_2·H_2O$, Zn_2SiO_4, $Ca_2ZnSi_2O_7$, $ZnFe_2O_4$, $ZnAl_2O_4$, metallic Zn, Cu_4Zn_6, $ZnSb_2O_6$, $ZnTiO_2$, and $Zn_{1-x}Al_x(OH)_2[SO_4]_{x/2} · n H_2O$. $CaZnCl_4$ is a synthesised reference with a structure that stoichiometrically should be $CaZnCl_4$. Still, since this compound is not included in the X-ray Diffraction (XRD) database, this could not be confirmed: no XRD peaks were found from the original compounds ($CaCl_2$ and $ZnCl_2$). Also, four references representing Zn adsorbed to surfaces were prepared, as Zn is known for its ability to be adsorbed to surfaces (Andersen et al., 2002; Struempler, 1973; Van Eynde et al., 2022): $Zn\_Fe_{10}O_{14}(OH)_2$, $Zn\_Al_2O_3 · 4 SiO_4·H_2O$, Zn_CaCO_3, and Zn_CaSO_4, where "Zn_" indicates that Zn is adsorbed. The reference materials were primarily selected for their relevance to untreated FA, rather than for the treated ashes specifically. This will affect the reliability of the results for the stabilised ashes.

2.4. XPS

The chemical analysis of FA particles was conducted using a PHI 5000 VersaProbe III Scanning XPS Microprobe (base pressure of $1 × 10^{-9}$ mbar). The excitation source was a monochromated Al operated at 25 W. The energy scale calibration was performed according to ISO 15472 standards, utilising reference core-level peaks of Au $4f_{7/2}$, Ag $3d_{5/2}$, and Cu $2p_{3/2}$ at 83.95 eV, 368.21 eV, and 932.64 eV, respectively.

The outermost surface features (~5 nm) were investigated by mounting a fine layer of particles on carbon tape, after which dry nitrogen gas was blown over the surface to remove loose particles. The sample was then loaded into the spectrometer, and the transfer procedure included exposure to vacuum for at least one hour before analysis. A dual-beam charge neutralisation system was utilised to prevent charge buildup for non-conductive materials.

Analysis points (3–6 points per sample) were selected based on scanning X-ray induced secondary electron imaging (SXI). Survey scans were performed in the range 0–1350 eV (pass energy 280 eV, step size 0.5 eV) for compositional analysis. High-resolution, narrow scans were performed in specific regions for chemical state analysis (pass energy, 26 eV; step size, 0.1 eV). The region spectra were fitted using the Multipak 9.7.0.1 software. Peak constraints regarding the area ratios and spin–orbit separation were defined as reported in the literature (Moulder et al., 1992). The peak areas of each element were normalised by the atomic sensitivity factors (ASF) provided by Multipak software in the quantitative analysis of the surface composition. Charge referencing was made to the adventitious C 1 s line at 284.8 eV to calibrate the binding energies of other elements. Selected region spectra were recorded, covering C 1 s, O 1 s, K 2p, Cl 2p, Si 2p, Zn L3M45M45, and Zn 2p, for chemical state identification. To capture the characteristics of the Zn 2p-region, data were collected in the energy range from 1015 to 1050 eV. The chemical state of Zn was investigated in detail using the NIST XPS–database (NIST, 2023). Furthermore, two reference compounds ($KZnCl_3$ and K_2ZnCl_4) were included in the analysis, as they

were not listed in the database but were deemed relevant to this study.

2.4.1. Surface enrichment factor

The relative Zn concentration in the ashes before and after treatment was evaluated using the surface enrichment factor (SEF), which quantifies the ratio of Zn on the particle surface compared to its bulk and is defined as $\frac{C_{surface}(wt\%)}{C_{bulk}(wt\%)}$. Each SEF value was determined by comparing the Zn concentration on the sample surface as measured by XPS with the bulk concentration derived from the total elemental analysis, presented in Table 1.

A SEF value equal to 1 indicates that the concentration of Zn on the surface is equal to that in the bulk. A factor greater than 1 implies enrichment of Zn on the surface relative to the bulk, whereas a value less than 1 indicates a depletion of Zn at the surface.

2.5. Chemical analytical methods

The total elemental compositions of selected elements in the untreated ash samples, i.e. GB2, GB4, GB5, and GB2APC, and the treated ash samples, i.e. GB2a, GB4a, GB5a and GB2APCg, were determined with inductively coupled plasma sector field mass spectrometry (ICP-SFMS). Before analysis, samples were digested according to ASTM D3682, ASTM D4503–08 (digestion using lithium metaborate (LiBO$_2$) and HNO$_3$) or SS-EN-13656 (digestion with HF, HNO$_3$, and HCl).

The metal concentrations following the sequential extractions were assessed by analysing the obtained liquids using X-ray fluorescence (XLAB 1000, Xepos 03). In addition, extractions following the first three steps in the sequence (MQ, Ac7 and Ac5) were analysed for pH (Seven2Go pH Meter, Mettler Toledo).

3. Results and discussion

3.1. Total elemental analysis

The total amounts of selected elements in the ash residues, i.e. after treatment, are given in Table 1. Additionally, the elemental enrichment or reduction compared to the untreated ash sample is shown. The total weight reduction after acid-leaching is 44 % for GB5, while the corresponding values for GB2 and GB4 are 57 % and 55 %, respectively. Ash samples GB2 and GB4 were treated with the three-cycle acid-leaching procedure, whereas GB5 underwent only one leaching cycle. Thus, the higher weight reduction for GB2a and GB4a is most likely due to the more aggressive leaching (pH < 1 vs 4), as discussed in Section 2.1.2 and Fig. 1, where a larger amount of the ash matrix is dissolved; however, variations in the ash matrix composition also influence dissolution (Rissler et al., 2024). Note that the weight reduction due to leaching will result in a relative mass enrichment in the residue for elements that do not leach, while elements efficiently leached are depleted. Consequently, e.g. Ba, Sn, and Ti, have more than 50 % higher contents in the treated ash samples, due to the low mobility of these elements and the release of salts and other easily soluble compounds, which cause total mass losses. This is especially pronounced in GB5a. Some of the enriched elements may be of interest for further recovery due to their high content and metal value, e.g., Ti (1–2 wt%), but they are likely bound in stable forms, indicating the need for advanced extraction methods.

The stabilised ash residue GB2APCg shows another pattern and has the overall lowest enrichment, as shown in Table 1, due to the addition of H$_2$SO$_4$ causing gypsum formation (CaSO$_4$·2 H$_2$O). The gypsum formation balances the weight loss resulting from the washing out of water-soluble compounds, resulting in a similar weight of the material after the treatment, i.e. no weight reduction, unlike the acidic treatment. As seen from Table 1, other elements than S are also enriched in the stabilised residue (e.g. Fe and V), which is related to the presence of these in the sulfuric acid used in this process.

3.2. Sequential extraction

The results, expressed as a percentage of the total contents, indicate a distinct decrease in the water-soluble fractions of Zn (fractions MQ and Ac7 in Fig. 2) after stabilisation and acid-leaching. This is likely related to the removal of chlorides, and is further supported by Table 1, which shows a decrease in total Cl concentration. As seen in Fig. 2, all treatment processes reduce the relative amount of Zn released in the exchangeable fraction (Ac7), from 30-55 % to less than 10 %. For the stabilisation process, i.e., GB2APCg, an increase is observed in the relative carbonate fraction (Ac5) from 25 % to 60 %. Smaller Zn amounts were released in the Ac5 fraction for all acid-leached samples compared to untreated, although this effect was less pronounced for the one-cycle leaching than for the three-cycle process. Acid-leaching increased the residual fraction in all samples.

Overall, the results indicate a shift in Zn speciation towards less mobile species following both treatments. The decrease in the exchangeable (Ac7) fraction seen in all samples is attributed to the removal of water-soluble species (e.g. chlorides), while the compounds soluble during reducible conditions remain. Furthermore, the acid-leached samples exhibit significant similarities in terms of Zn extractability, despite the different processes employed. The increase in the residual fraction for the acid-leached samples is related to the mass reduction following these treatments. The increase in water-soluble Zn observed after the three-cycle acid-leaching of GB2a and GB4a is most likely due to poor rinsing of the samples after treatment, but could also be attributed to chemical transformation and the precipitation of secondary compounds.

3.3. XANES

A comparison of the XANES spectra for untreated and treated ash reveals that both stabilisation and acid-leaching significantly alter the chemical speciation of Zn, as shown in Fig. 3. In the case of acid-leaching, the change in chemical form is most likely a result of the removal of water- and acid-soluble compounds, leaving behind the more stable Zn-forms. However, transformations may also occur. For the stabilised ash GB2APCg, the difference is due to alterations in the chemical composition, as the Zn content in the ash is not significantly decreased, as can be seen in Table 1.

To obtain information about the Zn-speciation, the XANES spectra of the untreated and treated ashes were analysed by linear combination fitting (LCF) using a library of XANES spectra from approximately 30 reference compounds, as described in (Rissler et al., 2024). An overview of the result is presented in Fig. 4.

The most obvious finding is that the untreated ashes initially contain a significant fraction of potassium zinc chlorides (K$_x$Zn$_y$Cl$_z$), ranging from 30 to 65 mol%, as was also concluded in earlier XANES studies of WtE ash (Rissler et al., 2024). The untreated ash with the lowest content of K$_x$Zn$_y$Cl$_z$ was the ash with lime additives, suggesting that some of the K$_x$Zn$_y$Cl$_z$ initially formed by condensation undergoes a chemical change when lime is present.

Following all treatments, the compound K$_x$Zn$_y$Cl$_z$ was either significantly reduced or completely removed. It remained only as a minor component (10 mol%) in the acid-leached samples GB2a and GB4a, as shown in Fig. 4. The remnants of water leachable Zn after the acid treatment are supported by the results from sequential leaching, which show that some water-soluble Zn remain in these two samples, while not in GB5a. This is likely due to poor rinsing and is further discussed in Sections 3.2 and 3.5. The LCF also indicates that Zn is present in the form of spinels (ZnFe$_2$O$_4$ and ZnAl$_2$O$_4$) and silicates (hemimorphite (Zn$_4$(Si$_2$O$_7$)(OH)$_2$·H$_2$O), willemite (Zn$_2$SiO$_4$), and Zn in glass) and that the relative content of these fractions increases in the samples that underwent acid-leaching, as expected when other soluble Zn-compounds were removed.

Comparing fits before and after stabilisation, i.e., GB2APC and

Table 1

Total contents of selected major and minor elements in treated ash samples GB2APCg (stabilisation), GB2a, GB4a, and GB5a (acid-leaching). The values are provided in mg/kg dry substance (DS). The elemental enrichment (EE) of each element in treated vs untreated ash samples is also provided. An EE value > 1 indicates that the content is higher in the treated ash, while an EE value < 1 means the content is lower. Contents $>\pm$ 0.2 of the treated ash samples are marked in yellow (enriched) and blue (depleted), respectively.

Element	GB2APCg		GB2a		GB4a		GB5a	
	Content [mg/kg DS]	EE*	Content [mg/kg DS]	EE*	Content [mg/kg DS]	EE*	Content [mg/kg DS]	EE*
Al	30 400	0.9	26 700	0.7	17 900	0.6	35 300	1.5
As	84	0.8	57	0.5	153	0.6	1 680	1.2
Ba	1 790	0.9	6 470	1.7	2 470	1.5	2 280	1.7
Ca	188 000	0.9	134 000	0.9	152 000	1.0	191 000	1.6
Cd	99	0.7	5.8	0.1	10	0.1	33	0.1
Co	37	1.3	78	0.8	13	0.8	35	1.4
Cl	89 700	0.6	5 550	0.1	2 740	0.1	7 640	< 0.1
Cr	496	1.4	821	1.3	403	1.3	916	1.6
Cu	1 740	0.9	1 170	0.6	155	0.2	2 730	1.1
Fe	35 700	2.0	20 000	0.9	16 500	1.0	16 900	1.7
K	19 400	0.6	8 590	0.2	10 100	0.2	10 700	0.2
Mg	15 300	1.1	5 520	0.4	3 100	0.3	10 700	1.1
Mn	915	1.0	421	0.4	378	0.4	729	1.3
Mo	43	0.9	82	1.5	29	2.4	52	1.8
Na	30 000	0.7	6 170	0.1	4 260	0.1	10 800	0.1
Ni	149	0.9	217	1.4	59	1.4	206	1.6
P	262	0.9	3 650	0.6	4 140	1.4	9 170	1.6
Pb	3 240	0.9	5 940	1.4	2 600	0.6	7 160	1.7
S	71 400	2.0	94 800	1.7	104 000	0.9	99 500	1.6
Sb	1 540	0.9	3 030	1.3	1 740	1.5	3 390	1.6
Si	86 500	1.0	181 000	1.5	196 000	1.4	73 500	1.4
Sn	584	0.9	1 400	1.8	1 310	1.9	2 650	1.7
Sr	321	0.9	562	1.3	573	1.1	433	1.5
Ti	13 200	1.3	19 700	1.7	11 900	1.8	12 900	1.8
V	262	2.8	57	0.4	23	0.4	56	1.5
Zn	14 400	0.9	7 250	0.4	7 120	0.4	20 400	0.5

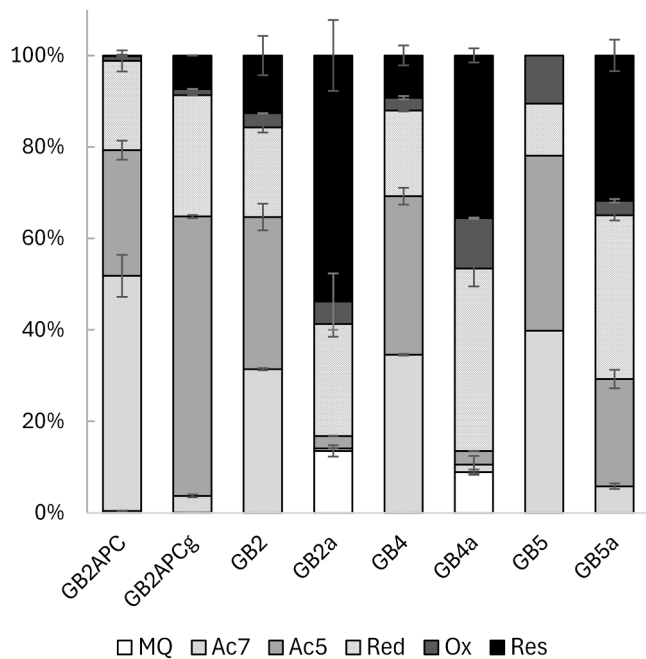*Calculated as [treated ash]/[untreated ash].

Fig. 2. Distribution of Zn in 6 different fractions according to the sequential extraction scheme in untreated and treated ash samples GB2APCg, GB2a, GB4a, and GB5a. MQ represents the extraction with deionised water; Ac7 corresponds to exchangeable species at pH 7; Ac5 corresponds to carbonates and easily soluble hydroxides released at pH 5; Red represents the reducible fraction (oxides), Ox represents the oxidizable fraction, and the remaining residue is referred to as Res. For further details, please refer to Section 2.2. Data for the original samples GB2, GB4, and GB5 are previously used in (Rissler et al., 2024). (For interpretation of the references to colour in this figure legend, the reader is referred to the web version of this article.)
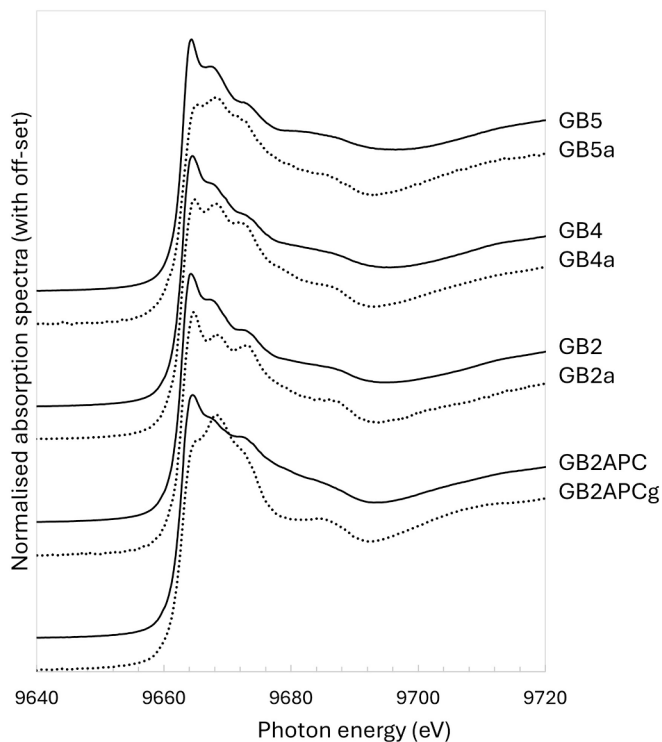

Fig. 3. XANES spectra at the Zn K-edge for ashes, before (solid lines) and after treatment (dotted lines). Spectra have been offset vertically for better visualisation.
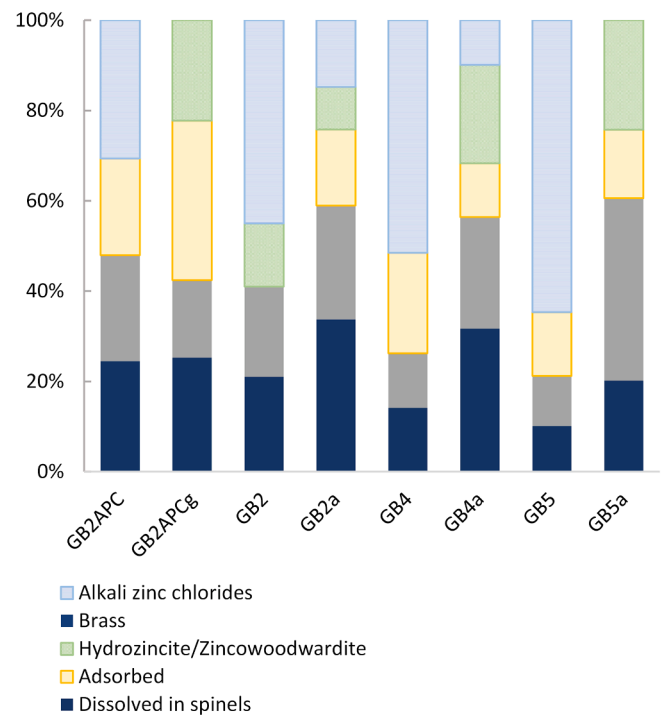

Fig. 4. Illustrating the Zn speciation from LCF of XANES spectra of the ash samples. The given fraction represents the molar fraction of the Zn bound in each type of chemical form. The interval fitted was -25 eV to $+35$ eV, where 0 eV corresponded to the absorption edge. Zn adsorbed to particle surfaces is here represented by the references given in the method section (2.3). Note that the results for GB2, GB4 and GB5 are the same as in Table 3 in Rissler et al. (2024) and are reported here for comparison purposes.

GB2APCg, shows consistency in the amount of Zn found as spinels and silicon oxides (in this case, the total Zn content remains the same before and after stabilisation). Other compounds that, according to the LCF, increase upon stabilisation are hydrozincite ($Zn_5(CO_3)_2(OH)_6$) and zincwoodwardite (($Zn_{1-x}Al_x)(OH)_2(SO_4)_{x/2} \cdot nH_2O$), while the potassium zinc chlorides disappear completely. Hydrozincite and zincwoodwardite are commonly found in similar environmental settings, typically formed as secondary minerals during the weathering and oxidation of zinc ores. Both minerals generally form under neutral to alkaline pH conditions and dissolve in acidic environments (Alwan and Williams, 1979; McMahon et al., 2019). However, the LCF of XANES data suggests their presence in the residue after acid-leaching. In the case of GB2, hydrozincite and zincwoodwardite appear to decrease during leaching, as would be expected. Please note that the apparent small decrease in Fig. 4 is much more pronounced than it appears here as the total Zn content is reduced by acid-leaching. However, for GB4 and GB5, the LCF results indicate formation of these phases during acid-leaching, which is inconsistent with their expected behaviour to dissolve at acidic conditions, making the LCF results questionable. Notably, the robustness of the fit for these compounds is lower compared to other phases that consistently appear across different fitting settings (e.g., energy calibration, normalisation parameters, and included reference spectra). The questionable LCF results for GB4 and GB5 are most likely due to the absence of critical Zn reference spectra for compounds formed during the acid leaching process. In their absence, the LCF algorithm substitutes these with other reference spectra with similar features, potentially leading to misidentification. Therefore, to improve the accuracy of XANES analysis for acid-leached samples, future work should focus on identifying and incorporating suitable Zn reference compounds specific to acid-leached ash into the reference database. It is also worth noting that the LCF method is limited to identifying phases present above a

certain concentration threshold (typically > 5 %), which can lead to the appearance of new compounds in the fit when others are removed, even if they were also present beforehand.

To further investigate the robustness of the results from the LCF analysis, the XANES spectra of the untreated ashes (GB2, GB4, and GB5) were fitted with the XANES spectra from the residues after acid-leaching and the reference compounds that were expected to be soluble at acidic pH. This analysis showed that about 20–30 % of the Zn in the fresh ash corresponds to Zn remaining in the residues after acid-leaching, i.e. 70–80 % of the Zn can be released during acid-leaching. This is in good agreement with the amount of Zn remaining in the ash after acid-leaching quantified by elemental analysis, as shown in Table 1.

While the LCF results indicate the chemical forms present, they should not be interpreted as precise speciation since that would require all relevant references to be included in the database used. The reference library used in this study is extensive compared to many earlier studies, but was originally developed in a project primarily focused on fresh ashes. Thus, the library would need to be expanded further to include more references relevant to the treated ashes. Therefore, the results from the LCFs for the treated ashes could be expected to be less certain. Furthermore, as the complexity of the mixture of Zn species increases, so does the uncertainty in the fit, with the increasing risk that a local minimum is found. Still, most of the results are robust and also in line with observations made by complementary techniques.

3.4. XPS

The surface compositions (wt% for selected elements) of the untreated and treated ash samples were determined by XPS. As expected, due to the high solubility of metal chlorides, the detected surface concentrations of Cl, K, and Zn were significantly reduced following acid-leaching, as reported in the Supplementary material, Table S3. This shows that $K_xZn_yCl_z$ have been effectively removed from the particle surfaces. This observation, in combination with the fact that XANES predicts a small fraction of $K_xZn_yCl_z$ remaining in GB2a and GB4a, suggests that the remaining $K_xZn_yCl_z$ is below the outermost particle surface, from which the compounds can still be leached by water during the sequential leaching. The XPS data also show that the surface concentrations of Ca, Fe, S, and Si increased after acid-leaching, suggesting that the remaining surface Zn is most likely bound in spinels and/or silicates, further supported by the XANES analysis. For the stabilised ash, a slight decrease in Zn surface concentration is observed, but otherwise, the composition remains similar.

To gain a deeper understanding of the change in surface-to-bulk distribution of different elements in the ash particles upon treatment, the relative surface composition was compared to the total elemental content using the surface enrichment factor (SEF), as presented in Table 2.

For all untreated ashes, Zn is enriched at the surface compared to the bulk. The decrease in surface-bound Zn after both leaching and stabilisation is reflected in the SEF values in Table 2 and the surface concentrations reported in Table S3. Ashes following acid-leaching show a higher decline in Zn at the surface compared to the ash following stabilisation. GB5a exhibits the highest concentration of Zn at the surface after acid-leaching, with a SEF slightly above 1. This could be attributed to the fact that this sample is leached only once, while GB2a and GB4a are leached in three steps. In contrast to GB2a and GB4a, all elements detected at the surface of GB5 are still present in GB5a, albeit at lower concentrations. A possible reason for certain elements, such as Cl, having similar or higher SEF-values than before acid-leaching is that small

Table 2
Surface enrichment factor (SEF) for selected elements in untreated and treated ashes. SEF around 1 indicates even distribution between surface and bulk, > 1 suggests surface enrichment, and < 1 indicates higher bulk concentration. SEF-values showing an increase (> 0.2) relative to the untreated ash are highlighted in yellow, while those showing a decrease (< 0.2) are highlighted in blue.

	GB2APC	GB2APCg	GB2	GB2a	GB4	GB4a	GB5	GB5a
Al	< DL	1.1	0.3	< DL	0.1	< DL	1.4	1.3
Ca	0.9	1.0	0.4	0.9	0.4	0.7	0.5	0.7
Cl	0.8	1.0	1.1	< DL	1.9	2.1	0.7	2.1
Cu	6.1	11.8	17.6	< DL	25.4	< DL	9.9	6.3
Fe	2.6	1.4	0.4	0.6	2.3	2.6	1.6	2.8
K	0.7	1.1	2.2	< DL	1.5	< DL	1.0	0.7
Na	1.0	1.2	1.6	< DL	1.9	< DL	1.1	1.7
Pb	2.6	1.7	7.5	< DL	8.8	4.5	5.3	3.3
S	1.5	0.7	1.6	1.2	1.1	1.0	0.8	0.7
Si	0.3	0.5	0.3	1.1	0.2	1.0	1.0	0.8
Zn	4.4	2.3	2.9	0.8	3.7	0.8	2.8	1.3

* DL = detection limit.

amounts are still concentrated at the outermost surface upon drying, despite a significant decrease in total content, as shown in Table 1.

In GB2APCg, most elements show SEF values close to 1, indicating an homogenous distribution between the surface and the bulk of the particles. Comparing the surface composition of GB2APC and GB2APCg reveals that the surface-bound Zn decreases but still remains enriched at the surface compared to the bulk.

The chemical state of Zn in the different ash samples was studied in more detail by analysing the Zn 2p-region, along with K 2p and Cl 2p. Fig. 5 illustrates the Zn 2p spectra for various ash fractions, showing the normalised intensity as a function of the binding energy. Data for two reference compounds, $KZnCl_3$ and K_2ZnCl_4, are included in the figure for comparison.

As shown in Fig. 5, the binding energy of the Zn 2p electrons of untreated ashes aligned better with K_2ZnCl_4 than with $KZnCl_3$, also supported by the XANES fitting, discussed in Figs. 2 and 4, respectively. The presence of K_2ZnCl_4 was confirmed through additional spectral analysis of several measurements in the untreated ash fractions, accompanied by a detailed analysis of the K 2p and Cl 2p regions. In addition to the presence of K_2ZnCl_4, the broad peaks indicate that multiple chemical states are present, suggesting that Zn exists in various chemical environments. The exact forms could not be identified, but components at lower binding energies are most likely due to the presence of mixed metal oxides and silicates, consistent with the results obtained by XANES. After careful investigation of K 2p and Cl 2p in GB2APCg, it was concluded that K_2ZnCl_4 is likely not present at the surface after stabilisation, meaning that Zn species undergo chemical transformation when subjected to stabilisation. Due to the low concentrations, determining the Zn chemical speciation in the acid-leached ashes was challenging. However, the lack of Zn at the surfaces indicates that Zn is incorporated in the bulk of the treated ashes. Any remaining $K_xZn_yCl_z$ in the ashes subjected to three acid-leaching cycles, as determined by XANES, are likely located beneath the sample surface.

As XPS only probes the outermost ~5 nm of the surface, the remaining $K_xZn_yCl_z$ compounds may either be located deeper within the particles or trapped in less accessible regions. In these cases, they remain exposed to acid-leaching but are undetectable by XPS, as emitted electrons cannot escape.

3.5. General discussion

The acid-leached ashes showed an enrichment (per ash mass unit) in the total amounts of Ca, Fe, and Si, and a depletion in the amounts of Cl, K, Na, and Zn compared to untreated ashes. The stabilised ash showed increased concentrations of Fe, S, and V, which are related to the acid used in the stabilisation process, as discussed in Section 3.1. The total content of Zn remained unaltered in the stabilised ash, while it decreased significantly in the acid-leached ashes. The relative decrease in Zn content is similar, although somewhat higher in the three-cycle acid-leached ashes. After leaching, the absolute Zn content is almost 3 times higher in GB5a compared to GB2a and GB4a, respectively. This suggests an opportunity to extract more Zn from the ash residue GB5a through additional acid-leaching cycles. However, efficiency is likely limited as large parts of Zn are available in non-leachable forms, as shown in Figs. 2 and 4.

The XPS data show that the surface concentration of Zn is reduced in the residue, as presented in Tables 2 and S3, and that when the easily soluble $K_xZn_yCl_z$ is removed from the surface, the relative abundance of e.g. Zn-silicates and spinels increases. XANES predicts a small fraction of $K_xZn_yCl_z$ in the bulk of the ashes after the three–cycle acid-leaching (GB2a and GB4a), which is shown in Fig. 4. This was confirmed by sequential leaching, where 10–15 % of the Zn was extracted in the initial fraction by MQ water. As discussed earlier, this could likely be avoided by additional rinsing. A possible explanation for this phenomenon is the non-optimal interaction between the acid and ash particles, caused by time limitations or physical aspects such as cracks and complex pore
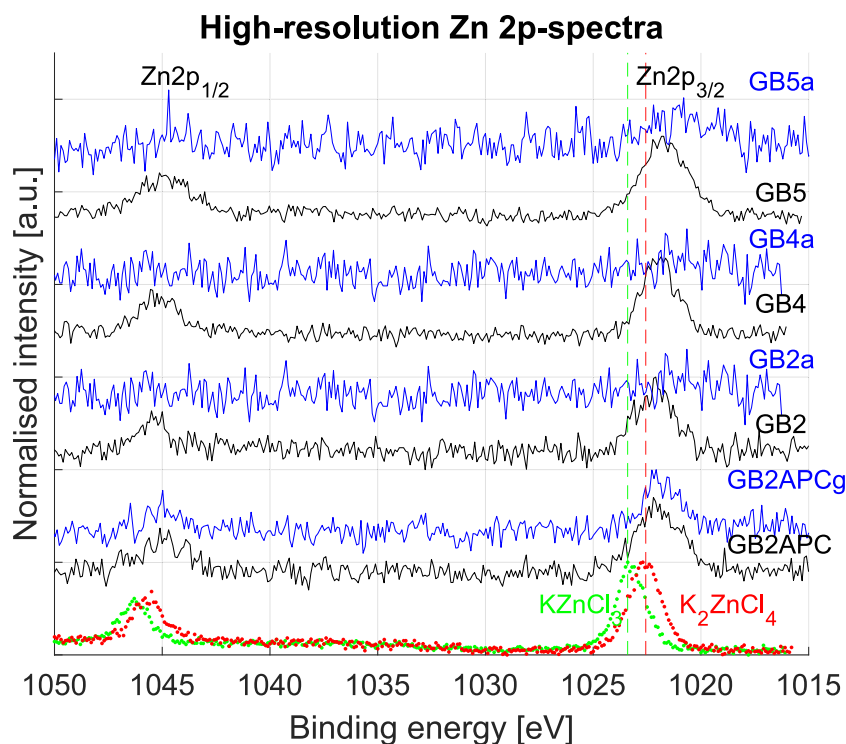

High-resolution Zn 2p-spectra

Fig. 5. High-resolution Zn 2p spectra. The figure highlights the differences in binding energies and peak shapes between different ash fractions. In addition, it emphasises the alignment with the reference compounds: untreated ash samples (black), treated ash samples (blue), and the reference compounds $KZnCl_3$ (green) and K_2ZnCl_4 (red). Spectra have been offset vertically for better visualisation. (For interpretation of the references to colour in this figure legend, the reader is referred to the web version of this article.)

structures in the ash. As a result, the mobilised ions are not completely transferred from the pore liquid into the bulk. Instead, they are adsorbed on particle surfaces and might reprecipitate, e.g. as $K_xZn_yCl_z$. The next time the ash is exposed to water or another liquid, these compounds may be released. This could also be the reason that acid-soluble compounds identified by XANES in the acid leached ashes, such as $ZnFe_2O_4$ (Zhang et al., 2018), are only partially removed during acid-leaching. However, another explanation for the presence of Zn in an iron spinel could be that these are stabilised by the additional substitution of transition elements for Fe in the magnetite structure (Liang et al., 2013). Even though Zn remains at the particle surfaces after stabilisation (GB2APCg), its chemical form has been altered.

Although the original ashes vary in composition and different treatment methods were used, all residues exhibit many similarities in terms of Zn leachability and speciation. The three treatments used effectively decrease the amount of easily soluble compounds, thereby revealing more stable Zn compounds, such as Zn-silicates and spinels. This suggests that the residues obtained from these treatments are not prone to leaching Zn if the rinsing of the residues is sufficient.

4. Conclusions

This study provides new insights into the Zn speciation in FA residues subjected to wet treatment processes, i.e. acid-leaching and stabilisation via gypsum formation, by uniquely employing spectroscopic techniques such as XANES and XPS. For the ash treated with acid-leaching, easily soluble Zn compounds, such as $K_xZn_yCl_z$ are efficiently released from the ash, and the remaining Zn is present in more stable compounds like spinels and silicates, compared to the untreated ashes. Low concentrations of easily soluble Zn compounds are still present in some of the residues, as confirmed by sequential extraction and XANES, but could not be identified on the particle surfaces by XPS. This is likely because the outermost layers of the particles are efficiently washed during the water washing steps used in all processes, while the washing is less efficient deeper within the particles due to factors such as cracks and complex pore structures. The Zn surface enrichment observed by XPS in the fresh ashes decreases with treatment. Altogether, thorough water washing is necessary after treatment to prevent unwanted Zn leaching from the ash residues.

The Zn content in the stabilised ash residue remains unchanged upon treatment. In contrast, the Zn contents are significantly lower in the acid-leached ash residues. A three-step acid-leaching process was applied to the two ashes, which, in an initial analysis of the raw ashes (using XANES and sequential leaching), indicated the presence of a higher fraction of more stable Zn compounds. This is based on the hypothesis that a stronger leaching would be needed to release Zn from the ashes. However, the use of a three-step acid-leaching process at pH < 1 did not release significantly more Zn compared to the one-step leaching at pH 4. This highlights the importance of studying the complex ash matrix using multiple techniques and methods, including advanced spectroscopic methods such as XANES and XPS, thereby enabling the development of resource- and energy-efficient processes that avoid unnecessary steps and chemicals.

To conclude, wet ash treatment yields more stable ash residues with respect to Zn, promoting the secondary use of the ash residues or safer landfilling. Acid-leaching is an effective method for recovering Zn from ash, but it requires well-designed procedures to achieve efficient full-scale processes.

CRediT authorship contribution statement

Karin Karlfeldt Fedje: Writing – review & editing, Writing – original draft, Investigation, Funding acquisition, Data curation, Conceptualization. **Ivana Staničić:** Writing – review & editing, Writing – original draft, Visualization, Methodology, Investigation, Formal analysis, Data curation. **Charlotte Nilsson:** Writing – review & editing, Writing – original draft, Visualization, Resources, Methodology, Investigation, Data curation. **Fanny Bergman:** Writing – review & editing, Writing – original draft. **Haakon M. Rui:** Writing – review & editing, Writing – original draft, Methodology, Conceptualization. **Inge Johansson:** Writing – review & editing, Writing – original draft, Methodology, Conceptualization. **Simone Sala:** Writing – review & editing, Writing – original draft. **Jenny Rissler:** Writing – review & editing, Writing – original draft, Visualization, Investigation, Funding acquisition, Formal analysis, Data curation, Conceptualization.

Declaration of competing interest

The authors declare that they have no known competing financial interests or personal relationships that could have appeared to influence the work reported in this paper.

Appendix A. Supplementary data

Supplementary data to this article can be found online at https://doi.org/10.1016/j.wasman.2025.115112.

Data availability

Data will be made available on request.

References

Alwan, A.K., Williams, P.A., 1979. Mineral formation from aqueous solution. Part I. The deposition of hydrozincite, Zn5(OH)6(CO3)2, from natural waters. Transit. Met. Chem. 4, 128–132. https://doi.org/10.1007/BF00618840/METRICS.

Andersen, M.K., Raulund-Rasmussen, K., Strobel, B.W., Hansen, H.C.B., 2002. Adsorption of cadmium, copper, nickel, and zinc to a poly(tetrafluorethene) porous soil solution sampler. J. Environ. Qual. 31, 168–175. https://doi.org/10.2134/JEQ2002.1680.

Chuai, X., Yang, Q., Zhang, T., Zhao, Y., Wang, J., Zhao, G., Cui, X., Zhang, Y., Zhang, T., Xiong, Z., Zhang, J., 2022. Speciation and leaching characteristics of heavy metals from municipal solid waste incineration fly ash. Fuel 328, 125338. https://doi.org/10.1016/J.FUEL.2022.125338.

De Matteis, C., Pollastri, S., Mantovani, L., Tribaudino, M., 2024. Potentially toxic elements speciation in bottom ashes from a municipal solid waste incinerator: A combined SEM-EDS, μ-XRF and μ-XANES study. Environ. Adv. 15, 100453. https://doi.org/10.1016/J.ENVADV.2023.100453.

de Repentigny, C., Courcelles, B., Zagury, G.J., 2018. Spent MgO-carbon refractory bricks as a material for permeable reactive barriers to treat a nickel- and cobalt-contaminated groundwater. Environ. Sci. Pollut. Res. 25, 23205–23214. https://doi.org/10.1007/s11356-018-2414-3.

Ferreira, C., Ribeiro, A., Ottosen, L., 2003. Possible applications for municipal solid waste fly ash. J. Hazard. Mater. 96, 201–216. https://doi.org/10.1016/S0304-3894(02)00201-7.

Karlfeldt Fedje, K., Andersson, S., 2020. Zinc recovery from Waste-to-Energy fly ash – A pilot test study. Waste Manag. 118, 90–98. https://doi.org/10.1016/J.WASMAN.2020.07.017.

Karlsson, S., Allard, B., Håkansson, K., 1988. Chemical characterization of stream-bed sediments receiving high loadings of acid mine effluents. Chemical Geology 67, 1–15. https://doi.org/10.1016/0009-2541(88)90002-2.

Klementiev, K., Norén, K., Carlson, S., Sigfridsson Clauss, K.G.V., Persson, I., 2016. The BALDER beamline at the MAX IV laboratory. J. Phys. Conf. Ser. 712, 012023. https://doi.org/10.1088/1742-6596/712/1/012023.

Liang, D., Wang, F., Lv, G., 2023. The resource utilization and environmental assessment of MSWI fly ash with solidification and stabilization: A review. Waste Biomass Valoriz. 15 (1), 37–56. https://doi.org/10.1007/S12649-023-02275-5.

Liang, X., Zhong, Y., Tan, W., Zhu, J., Yuan, P., He, H., Jiang, Z., 2013. The influence of substituting metals (Ti, V, Cr, Mn, Co and Ni) on the thermal stability of magnetite. J. Therm. Anal. Calorim. 111, 1317–1324. https://doi.org/10.1007/S10973-012-2432-1/FIGURES/6.

McMahon, M.E., Santucci, R.J., Scully, J.R., 2019. Advanced chemical stability diagrams to predict the formation of complex zinc compounds in a chloride environment. RSC Adv. 9, 19905–19916. https://doi.org/10.1039/C9RA00228F.

Moulder, J., Stickle, W., Sobol, W., Bomben, K.D., 1992. Handbook of X-Ray Photoelectron Spectroscopy.

NIST, 2023. NIST X-ray Photoelectron Spectroscopy Database. https://doi.org/https://srdata.nist.gov/xps/.

Quina, M.J., Bontempi, E., Bogush, A., Schlumberger, S., Weibel, G., Braga, R., Funari, V., Hyks, J., Rasmussen, E., Lederer, J., 2018. Technologies for the management of MSW incineration ashes from gas cleaning: New perspectives on recovery of secondary raw materials and circular economy. Sci. Total Environ. 635, 526–542. https://doi.org/10.1016/J.SCITOTENV.2018.04.150.

Rasmussen, E., 2015. Sambehandling af RGA og scrubbervaeske fra forbraendingsanlaeg med HALOSEP processen. https://doi.org/https://www2.mst.dk/Udgiv/publikationer/2015/02/978-87-93283-72-5.pdf.

Ravel, B., Newville, M., 2005. ATHENA, ARTEMIS, HEPHAESTUS: data analysis for X-ray absorption spectroscopy using IFEFFIT. urn:issn:0909-0495. https://doi.org/10.1107/S0909049505012719.

Renova AB, 2023. WHERE WASTE BECOMES HEAT AND ELECTRICITY Sävenäs Waste-to-Energy plant, Gothenburg. https://doi.org/https://www.renova.se/globalassets/06.-om-oss/koncern/trycksaker/230613_where_waste_becomes_heat_and_electricity_digital.pdf.

Rissler, J., Fedje, K.K., Klementiev, K., Ebin, B., Nilsson, C., Rui, H.M., Klufthaugen, T.M., Sala, S., Johansson, I., 2024. Zinc speciation in fly ash from MSWI using XAS - novel insights and implications. J. Hazard Mater. 477, 135203. https://doi.org/10.1016/J.JHAZMAT.2024.135203.

Rissler, J., Klementiev, K., Dahl, J., Steenari, B.M., Edo, M., 2020. Identification and quantification of chemical forms of Cu and Zn in MSWI ashes using XANES. Energy Fuels 34, 14505–14514. https://doi.org/10.1021/ACS.ENERGYFUELS.0C02226/ASSET/IMAGES/LARGE/EF0C02226_0004.JPEG.

Robert, A., Cerenius, Y., Tavares, P.F., Hultin, A., Stigenberg, Karis, O., Lloyd Whelan, A. C., Runéus, C., Thunnissen, M., 2023. MAX IV Laboratory. Eur. Phys. J. Plus 138 (6), 1–10. https://doi.org/10.1140/EPJP/S13360-023-04018-W.

Rui, H.M.V., Gerhardsen, M., Breinholt Jensen, M., Marki, T., Ulltang, T., 2021. Method and apparatus for neutralizing and stabilizing of fly ash.

Schlumberger, S., Schuster, M., Ringmann, S., Koralewska, R., 2007. Recovery of high purity zinc from filter ash produced during the thermal treatment of waste and inerting of residual materials. Waste Manage. Res. 25, 547–555. https://doi.org/10.1177/0734242X07079870.

Scholz, P., Vogel, C., Schuck, G., Simon, F.G., 2024. Speciation of copper and zinc compounds relevant for the hazard property (HP) 14 classification of municipal solid waste incineration bottom and fly ashes. Waste Manage. 189, 421–426. https://doi.org/10.1016/J.WASMAN.2024.09.001.

Staničić, I., Backman, R., Cao, Y., Rydén, M., Aronsson, J., Mattisson, T., 2022. Fate of trace elements in Oxygen Carrier Aided Combustion (OCAC) of municipal solid waste. Fuel 311, 122551. https://doi.org/10.1016/J.FUEL.2021.122551.

Struempler, A.W., 1973. Adsorption characteristics of silver, lead, cadmium, zinc, and nickel on borosilicate glass, polyethylene, and polypropylene container surfaces. Anal Chem 45, 2251–2254. https://doi.org/10.1021/AC60335A014.

Struis, R.P.W.J., Ludwig, C., Lutz, H., Scheidegger, A.M., 2004. Speciation of zinc in municipal solid waste incineration fly ash after heat treatment: An X-ray absorption spectroscopy study. Environ. Sci. Technol. 38, 3760–3767. https://doi.org/10.1021/ES0346126.

Tessier, A., Campbell, P.G.C., Bisson, M., 1979. Sequential extraction procedure for the speciation of particulate trace metals. Anal. Chem. 51, 844–851. https://doi.org/10.1021/AC50043A017/ASSET/AC50043A017.FP.PNG_V03.

United Nations Environment, Association, I.S.W.P., 2024. Global Waste Management Outlook 2024 - Beyond an age of waste: Turning rubbish into a resource. Global Waste Manage. Outlook 2024, 18–21.

Van Eynde, E., Hiemstra, T., Comans, R.N.J., 2022. Interaction of Zn with ferrihydrite and its cooperative binding in the presence of PO4. Geochim Cosmochim Acta 320, 223–237. https://doi.org/10.1016/J.GCA.2022.01.010.

Wu, Q., Wu, Z., Wu, H., Wang, Q., Huang, N., Zhou, J., Li, X., Shi, L., Tian, S., Li, M., 2023. Thermal treatment of municipal solid waste incineration fly ash and nanofiltration membrane concentrate co-processing: Speciation of chromium and its leachability. J. Clean Prod. 398, 136619. https://doi.org/10.1016/J.JCLEPRO.2023.136619.

Zhang, S., Shi, R., Tan, Y., 2018. Comparison of the solubility of ZnFe2O4, Fe3O4 and Fe2O3 in high temperature water. J. Solution Chem. 47, 1112–1126. https://doi.org/10.1007/S10953-018-0779-Z/FIGURES/3.